Figure 1: OH IR (0.9-1.7μm) all-sky airglow imager.

Analyzing Atmospheric Gravity Waves Over Antarctica and Visualizing Machine Learning Data

Anastasia Brown, Kenneth Zia, Pierre-Dominique Pautet, Yucheng Zhao, Connor Waite, Dallin Tucker, Eli Kroeber, Max Haehnel, and Michael J. Taylor

Utah State University Physics Department, Center for Atmospheric and Space Sciences

ANtarctic Gravity Wave Instrument Network (ANGWIN)

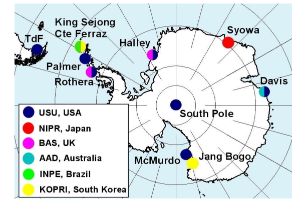

Figure 2: ANGWIN imager network map.

Introduction

Gravity Waves are buoyancy waves that propagate in the atmosphere [Matsuda et al., 2014]

- Mostly generated by tropospheric weather,
- Can vertically propagate above 100 km altitude,
- Affect the temperature structure of the atmosphere,
- Drive pole-to-pole circulation.

ANGWIN (Fig. 1 & 2)

- An international collaboration, investigates the upper atmosphere dynamics over a continent-size region, uses a network of all-sky imagers.
- Large data sets (~1M images per winter) --> bottle neck.

Algorithm used:

- Light Gradient Boosted Machine (LightGBM) [Ke et al., 2017],
- Fast but requires unique models for each station.
- Inspire by ML model used to sort Themis Aurora all sky imager data [Clausen et al., 2018]: "Clean" (0),"Obscured" (1).

Research goals:

- **Compare validated Halley models' findings,**
- **Compare short period gravity waves power over different Antarctic stations.**

Method

Use LightGBM Models to identify "clean" windows (Fig. 3)

- 2 hours of "clean" data,
- 3 minutes or less between each "clean" data point.

Compare window identification methods

- Manually identified windows vs computationally identified,
- Window length, OH power (Fig. 6).

Compare filtered vs unfiltered computationally found windows

- Subtracted phase velocity spectrums (Fig. 5).

Process FFT spectrum analysis to study atmospheric gravity waves [Matsuda et al., 2014]

- Performed on "clean", processed windows (Fig. 4),
- Generates gravity wave phase velocity spectrums.

Image Processing

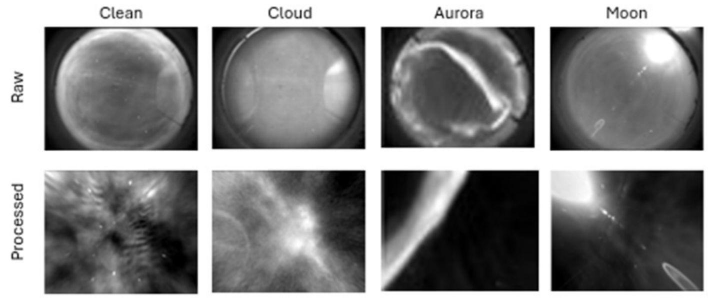

Figure 3: "Clean" windows are defined as free of excessive cloud, aurora, moon, or twilight contamination.

Subtracted phase velocity spectrums

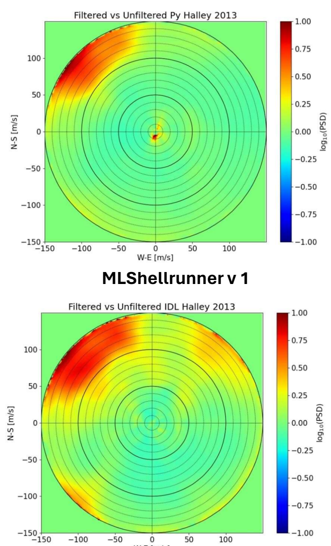

Figure 5: Difference between the monthly averaged phase velocity spectrums generated using manually verified "clean" windows and those using all windows found.

Differences between windows

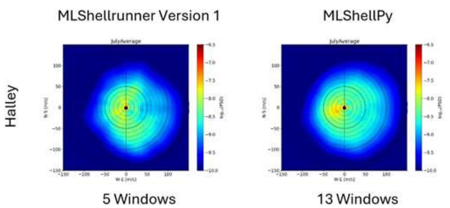

Figure 4: Monthly power spectrums processed with the clean windows found by MLShellrunner v1 (left) vs found by MLShellPy (right). The number and length of windows change across identification methods which affect monthly average phase velocity spectrums.

Results

Window selection method [Fig. 5]

- Windows flagged by MLShellPy contain less error around the edges than MLShellrunner Version 1, but the centers remain comparable.

Average power and window length [Fig. 6]

- Average power measured at Davis is approximately 4.6x larger than Halley's and 4.8x larger than McMurdo's,
- Station with the longest windows: Halley. Station with the most windows: McMurdo.

Phase Velocity Spectrum [Fig. 7]

- Power increases over the course of the winter for all the stations and directionality is very similar for McMurdo and Davis (~SW) during most of the winter. It varies for Halley from W to E, which was unexpected.

Window length and power station comparison 2013

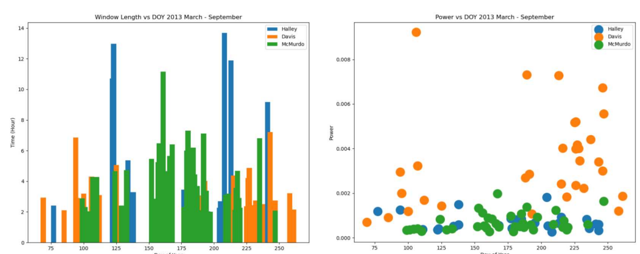

Figure 6 Comparison of average power and length of window between the Halley, Davis, and McMurdo stations. Windows gathered using MLShellrunner Version 1.

Phase velocity spectrum station comparison

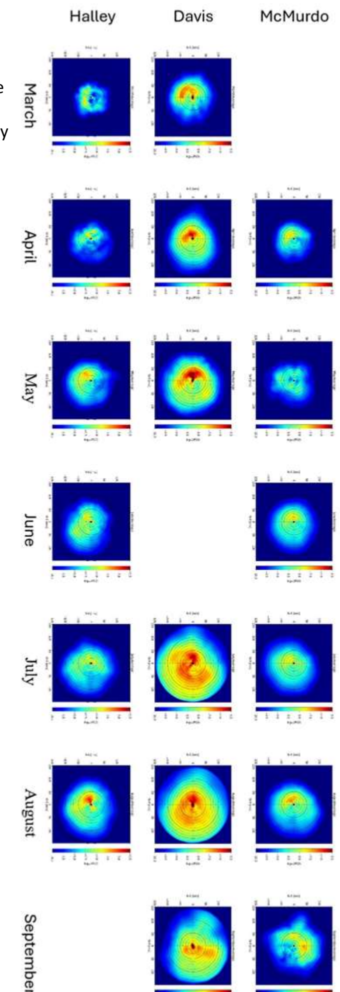

Figure 7: Monthly averaged phase velocity spectrums from Halley, Davis, and McMurdo generated by manually verified "clean" windows found by MLShellrunner Version 1 for an entire season.

Conclusion

- Machine learning in ASI cleaning removes the bottle neck created by the large data set.
- The number of clean windows correctly identified by the Halley model comparable to that of Davis and McMurdo.
- Machine-identified windows and manually identified windows shows similar results.
- More "clean" windows may be found using MLShellPy window flagging algorithm as opposed to the original MLShellrunner version 1 algorithm.

References and Acknowledgments

[1] Matsuda, T. S., T. Nakamura, M. K. Ejiri, M. Tsutsumi, and K. Shiokawa (2014), New statistical analysis of the horizontal phase velocity distribution of gravity waves observed by airglow imaging, *J. Geophys. Res. Atmos.*, 119, 9707–9718, doi:10.1002/2014JD021543.

Zia, Kenneth I., "Investigating Atmospheric Gravity Waves Using 3-Dimensional Spectral Analysis" (2022). *All Graduate Theses and Dissertations, Spring 1920 to Summer 2023*. 8645. https://digitalcommons.usu.edu/etd/8645

Guolin Ke1 , Qi Meng2 , Thomas Finley3 , Taifeng Wang1 , Wei Chen1 , Weidong Ma1 , Qiwei Ye1 , Tie-Yan Liu1, "LightGBM: A Highly Efficient Gradient Boosting Decision Tree", *NeurIPS Proceedings*. *https://proceedings.neurips.cc/paper_files/paper/2017/file/6449f44a102fde848669bdd9eb6b76fa-Paper.pdf*

Clausen, L. B. N., & Nickisch, H. (2018). Automatic classification of auroral images from the Oslo Auroral THEMIS (OATH) data set using machine learning. Journal of Geophysical Research: Space Physics, 123, 5640– 5647. https://doi.org/10.1029/2018JA025274

Matsuda, T. S., T. Nakamura, M. K. Ejiri, M. Tsutsumi, Y. Tomikawa, M. J. Taylor, Y. Zhao, P.-D. Pautet, D. J. Murphy, and T. Moffat-Griffin (2017), Characteristics of mesospheric gravity waves over Antarctica observed by Antarctic Gravity Wave Instrument Network imagers using 3-D spectral analyses, *J. Geophys. Res. Atmos.*, 122, 8969–8981, doi:10.1002/2016JD026217.

Acknowledgments: This research project is supported by NSF grant 2029318.